

## Syntheses and Crystal Structures of Two Topologically Related Modifications of $\text{Cs}_2[(\text{UO}_2)_2(\text{MoO}_4)_3]$

S. V. Krivovichev

Department of Crystallography, St. Petersburg State University, St. Petersburg 199034, Russia

C. L. Cahill\*

Department of Chemistry, George Washington University, Washington, D.C. 20052

P. C. Burns

Department of Civil Engineering and Geological Sciences, University of Notre Dame, Notre Dame, Indiana 46556

Received March 28, 2001

Two polymorphs of  $\text{Cs}_2(\text{UO}_2)_2(\text{MoO}_4)_3$  have been synthesized by hydrothermal ( $\alpha$ -phase) and high-temperature ( $\beta$ -phase) routes. Both were characterized by single-crystal X-ray diffraction:  $\alpha$ - $\text{Cs}_2(\text{UO}_2)_2(\text{MoO}_4)_3$ , orthorhombic,  $Pna2_1$ ,  $a = 20.4302(15)$  Å,  $b = 8.5552(7)$  Å,  $c = 9.8549(7)$  Å,  $Z = 4$ ;  $\beta$ - $\text{Cs}_2(\text{UO}_2)_2(\text{MoO}_4)_3$ , tetragonal,  $P4_2/n$ ,  $a = 10.1367(8)$  Å,  $c = 16.2831(17)$  Å,  $Z = 4$ . The structures of both phases consist of linked  $\text{UO}_7$  pentagonal bipyramids and  $\text{MoO}_4$  tetrahedra:  $\alpha$ - $\text{Cs}_2(\text{UO}_2)_2(\text{MoO}_4)_3$  is a framework compound with large channels parallel to the  $c$  axis. Two cesium sites are located in these channels and are coordinated by 8 and 10 oxygen atoms. The structure of  $\beta$ - $\text{Cs}_2(\text{UO}_2)_2(\text{MoO}_4)_3$  contains corrugated  $[(\text{UO}_2)_2(\text{MoO}_4)_3]$  sheets that are parallel to (001). The cesium cations are located between the sheets and are coordinated by eight oxygen atoms. The structures are topologically related; both can be described in terms of chains of 5-connected  $\text{UO}_7$  pentagonal bipyramids and 3- and 4-connected  $\text{MoO}_4$  tetrahedra.

### Introduction

The pursuit of novel porous and layered materials is currently of great interest due to the applicability of these compounds (zeolites, aluminophosphates, mesoporous oxides, sulfides, coordination solids, etc.) in areas such as heterogeneous catalysis, ion-exchange, gas storage and separation, sensors, and radioactive waste remediation.<sup>1–4</sup> One prospective class of materials in this direction is the uranium oxide and fluoride compounds that show a great variety of layered and framework structures.<sup>5–11</sup> A survey of the crystal chemistry of hexavalent uranium oxide

compounds shows that U(VI) most commonly occurs as an approximately linear uranyl cation,  $\text{UO}_2^{2+}$ , that is coordinated by four to six equatorial anions.<sup>12,13</sup> Whereas the bonding requirements of the apical anion positions are close to satisfied from the bond-valence theory viewpoint,<sup>14–16</sup> the equatorial anions require significant additional bonding. This

\* Corresponding author. E-mail: cahill@gwu.edu.

- (1) Cheetham, A. K.; Férey, G.; Loiseau, T. *Angew. Chem., Int. Ed. Engl.* **1999**, *38*, 3268–3292.
- (2) Corma, A. *Chem. Rev.* **1997**, *97*, 2373–2420.
- (3) Dyer, A. *An Introduction to Zeolite Molecular Sieves*; John Wiley and Sons: 1988.
- (4) Barton, T. J.; Bull, L. M.; Klemperer, W. G.; Loy, D. A.; McEnaney, B.; Misono, M.; Monson, P. A.; Pez, G.; Scherer, G. W.; Vartuli, J. C.; Yaghi, O. M. *Chem. Mater.* **1999**, *11*, 2633–2656.

- (5) Almond, P. M.; Deakin, L.; Porter, M. J.; Mar, A.; Albrecht-Schmitt, T. E. *Chem. Mater.* **2000**, *12*, 3208–3213.
- (6) Almond, P. M.; Deakin, L.; Mar, A.; Albrecht-Schmitt, T. E. *Inorg. Chem.* **2001**, *40*, 886–890.
- (7) Cahill, C. L.; Burns, P. C. *Inorg. Chem.* **2001**, *40*, 1347–1351.
- (8) Francis, R. J.; Halasyamani, P. S. *Angew. Chem., Int. Ed. Engl.* **1998**, *37*, 2214–2217.
- (9) Francis, R. J.; Halasyamani, P. S.; Bee, J. S.; O'Hare, D. *J. Am. Chem. Soc.* **1999**, *121*, 1609–1610.
- (10) Walker, S. M.; Halasyamani, P. S.; Allen, S.; O'Hare, D. *J. Am. Chem. Soc.* **1999**, *121*, 10513–10521.
- (11) Talley, C. E.; Bean, A. C.; Albrecht-Smith, T. E. *Inorg. Chem.* **2000**, *39*, 5174–5175.
- (12) Burns, P. C. *Rev. Mineral.* **1999**, *38*, 23–90.
- (13) Burns, P. C.; Miller, M. L.; Ewing, R. C. *Can. Mineral.* **1996**, *34*, 845–880.
- (14) Brese, N. E.; O'Keeffe, M. *Acta Crystallogr.* **1991**, *B47*, 192–197.

results in the tendency of uranyl polyhedra to polymerize to form sheet structures. In fact, of the 65  $U^{6+}-O$  minerals with known structures, 50 have layered topologies.<sup>12</sup>

To offset the predisposition of uranyl compounds toward layered structures, and to direct the formation of framework phases, flexible M–O linkages can be incorporated to effectively separate the U–O structural building units from one another. The  $Mo^{6+}$  cation is of special interest in this regard, due to the range of observed U–O–Mo bond angles. As a result, there are many uranyl molybdates with both layered<sup>17–23</sup> and framework<sup>24–30</sup> structures. Within these phases, the most common coordination polyhedra for Mo(VI) and U(VI) are  $MoO_4$  tetrahedra and  $UO_7$  pentagonal bipyramids, respectively. These polyhedra link to each other via common vertexes to produce a large variety of complex uranyl molybdate oxyanions, ranging from finite clusters through chains and sheets to frameworks.

The current study involves the Cs–U–Mo–O system, which has been the focus of several authors using various experimental techniques.<sup>21,29,31–33</sup> To date, structural studies have been reported only for two Cs–Mo–U compounds,  $Cs_2UO_2(MoO_4)_2 \cdot H_2O$  and  $Cs_2[(UO_2)_6(MoO_4)_7(H_2O)_2]$ .<sup>21,29</sup> This family of materials is of particular interest because they may be important for the long-term evolution of a geological repository for nuclear waste. Recently, Buck et al.<sup>30</sup> discovered  $(Cs_{2-x}Ba_{1-x})[(UO_2)_5(MoO_6)(OH)_6] \cdot nH_2O$  ( $x \sim 0.4$ ,  $n \sim 6$ ) formed due to the alteration of spent nuclear fuel during hydrologically unsaturated tests designed to simulate conditions expected in the proposed nuclear waste repository at Yucca Mountain, NV. Several other recent studies have shown that uranyl phases formed due to the alteration of nuclear waste may incorporate various radionuclides into their structures, thus potentially impacting the release of these

species into the biosphere.<sup>34–38</sup> In this paper we report the syntheses, structures, and thermal properties of two novel, isochemical cesium uranyl molybdates:  $\alpha$ - and  $\beta$ - $Cs_2[(UO_2)_2(MoO_4)_3]$ . The  $\alpha$  phase possesses a novel framework and was synthesized hydrothermally, whereas the  $\beta$  phase is a layered material formed by melting the  $\alpha$  phase or from high-temperature synthesis.

## Experimental Section

**Synthesis.** The  $\alpha$ - $Cs_2[(UO_2)_2(MoO_4)_3]$  phase was synthesized in a Teflon-lined steel autoclave by combining 0.06 g of Cs(OOCCH<sub>3</sub>) (Alfa), 0.04 g of  $UO_2(CH_3COO)_2 \cdot 2H_2O$  (Alfa), 0.04 g  $MoO_3$  (Sigma), and 5.0 g of ultrapure  $H_2O$  (molar ratio Cs:U:Mo: $H_2O$  = 3:3:1:1000). This mixture (pH = 5.14) was held static at 180 °C for 7 days, followed by cooling to room temperature over 2 h. The product, a yellow solid, was collected by filtration and washed with EtOH and  $H_2O$  and allowed to dry in air. The phase crystallized as blade-shape greenish-yellow crystals. Reactions consistently resulted in pure phases (as determined via powder diffraction, below) with yields of approximately 70% based on U.

The  $\beta$ - $Cs_2[(UO_2)_2(MoO_4)_3]$  phase was originally obtained by melting  $\alpha$ - $Cs_2[(UO_2)_2(MoO_4)_3]$  and allowing the liquid to crystallize (see below). It was subsequently synthesized as follows: a ground mixture of 0.192 g of Cs(OOCCH<sub>3</sub>), 0.143 g  $UO_3$  (Alfa) and 0.144 g  $MoO_3$  was heated in a corundum crucible to 850 °C for 2 h. The mixture was then cooled to 650 °C over 5 h and held at 650 °C for 2 h, followed by cooling to 350 °C over 50 h and finally to room temperature over 22 h. Yellow, plate-shaped crystals were obtained.

**Thermal Analysis.** Simultaneous DTA/TGA analyses were performed on  $\alpha$ - $Cs_2[(UO_2)_2(MoO_4)_3]$  using a TA Instruments SDT 2960 to check for any occluded volatile species not found in the X-ray analysis. A heating cycle under flowing nitrogen from 25 to 800 °C (10 °/min) indicated no significant weight loss. The sample demonstrated thermal stability until approximately 750 °C, at which point melting was observed. Upon cooling, recrystallization occurred at approximately 650 °C. A powder XRD analysis (below) of the post-TGA sample indicated that the phase was  $\beta$ - $Cs_2[(UO_2)_2(MoO_4)_3]$  (Powder Diffraction File No. 41-145).<sup>32</sup>

**X-ray Powder Diffraction.** Powder diffraction data for both  $\alpha$ - and  $\beta$ - $Cs_2[(UO_2)_2(MoO_4)_3]$  were collected using a Rigaku Miniflex diffractometer (Cu  $K\alpha$ , 3–60° in  $2\theta$ ). The diffractograms were compared to the calculated patterns (Palmer, 1999, No. 38). No other detectable crystalline phases were present in either the  $\alpha$  or  $\beta$  samples. The powder diffraction pattern for  $\beta$ - $Cs_2[(UO_2)_2(MoO_4)_3]$  is identical to PDF 41-145.

**Electron Probe Microanalysis.** A single crystal of NDU-1 was mounted in epoxy, polished, and coated with carbon. Electron microprobe analyses were done using a JEOL 733 operated in wavelength-dispersive spectroscopy (WDS) mode. All analyses were performed with an accelerating voltage of 15 kV and a probe current of 25 nA, with a defocused beam size of 10  $\mu m$  in diameter. The average of four analyses (at. wt %) is Cs 18.3%, U: 35.8% Mo 22.4%, and O 23.5% (by difference), which is in good agreement with the theoretical values, calculated on the basis of

- (15) Brown, I. D. *Structure and Bonding*; Academic Press: New York, 1981.
- (16) Brown, I. D. *Acta Crystallogr.* **1997**, *B53*, 381–393.
- (17) Lee, M. R.; Jaulmes, S. J. *Solid State Chem.* **1987**, *67*, 364–368.
- (18) Marsh, R. E. J. *Solid State Chem* **1988**, *73*, 577–578.
- (19) Sadikov, G. G.; Krasovskaya, T. I.; Polyakov, Y. A.; Nikolaev, V. P. *Izv. AN SSSR, Neorg. Mater.* **1988**, *24*, 109–115.
- (20) Halasyamani, P. S.; Francis, R. J.; Walker, S. M.; O'Hare, D. *Inorg. Chem.* **1999**, *38*, 271–279.
- (21) Rastsvetaeva, R. K.; Barinova, A. V.; Fedoseev, A. M.; Budantseva, N. A.; Nekrasov, Y. V. *Dokl. Chem* **1999**, 52–55.
- (22) Krivovichev, S. V.; Burns, P. C. *Can. Mineral.* **2000**, *38*, 717–726.
- (23) Khrestalev, V. N.; Andreev, G. B.; Antipin, M. Y.; Fedoseev, A. M.; Budantseva, N. A.; Shirokova, I. B. *Zh. Neorg. Khim.* **2000**, *45*, 1996–1998.
- (24) Serezhkin, V. N.; Trunov, V. K.; Makarevich, L. G. *Kristallografiya* **1980**, *25*, 858–860.
- (25) Tabachenko, V. V.; Kovba, L. M.; Serezhkin, V. N. *Sov. J. Coord. Chem.* **1983**, *9*, 886–889.
- (26) Tabachenko, V. V.; Kovba, L. M.; Serezhkin, V. N. *Sov. J. Coord. Chem.* **1984**, *10*, 311–315.
- (27) Tabachenko, V. V.; Balashov, V. L.; Kovba, L. M.; Serezhkin, V. N. *Sov. J. Coord. Chem.* **1984**, *10*, 471–474.
- (28) Tali, R.; Tabachenko, V. V.; Kovba, L. M.; Dem'yanetz, L. N. *Zh. Neorg. Khim.* **1994**, *39*, 1752–1754.
- (29) Krivovichev, S. V.; Burns, P. C. *Can. Mineral.* **2001**, *38*, in press.
- (30) Buck, E. C.; Wronkiewicz, D. J.; Finn, P. A.; Bates, J. K. *J. Nucl. Mater.* **1997**, *249*, 70–76.
- (31) Krasovskaya, T. I.; Polyakov, Y. A.; Rozanov, I. A. *Izv. AN SSSR, Neorg. Mater.* **1980**, *16*, 1824–1828.
- (32) Serezhkin, V. N.; Tatarinova, E. H.; L. B., S. *Zh. Neorg. Khim* **1987**, *32*, 227–229.
- (33) Misra, N. L.; Chawla, K. L.; Venugopal, V.; Jayadevan, N. C.; Sood, D. D. *J. Nucl. Mater.* **1995**, *226*, 120–127.

- (34) Burns, P. C.; Ewing, P. C.; Miller, M. L. *J. Nucl. Mater.* **1997**, *245*, 1–9.
- (35) Burns, P. C.; Finch, R. J.; Hawthorne, F. C.; Miller, M. L.; Ewing, R. C. *J. Nucl. Mater.* **1997**, *249*, 199–206.
- (36) Burns, P. C. *J. Nucl. Mater.* **1999**, *265*, 218–223.
- (37) Chen, F.; Burns, P. C.; Ewing, R. C. *J. Nucl. Mater.* **1999**, *275*, 81–94.
- (38) Chen, F.; Burns, P. C.; Ewing, R. C. *J. Nucl. Mater.* **2000**, *278*, 225–232.

**Table 1.** Crystal Data and Structure Refinement for  $\alpha$ - and  $\beta$ -Cs<sub>2</sub>[(UO<sub>2</sub>)<sub>2</sub>(MoO<sub>4</sub>)<sub>3</sub>]

	$\alpha$ -Cs <sub>2</sub> [(UO <sub>2</sub> ) <sub>2</sub> (MoO <sub>4</sub> ) <sub>3</sub> ]	$\beta$ -Cs <sub>2</sub> [(UO <sub>2</sub> ) <sub>2</sub> (MoO <sub>4</sub> ) <sub>3</sub> ]
chem formula	Cs <sub>2</sub> U <sub>2</sub> Mo <sub>3</sub> O <sub>16</sub>	Cs <sub>2</sub> U <sub>2</sub> Mo <sub>3</sub> O <sub>16</sub>
fw	1285.62	1285.62
<i>T</i> , K	293(2)	293(2)
$\lambda$ , Å	0.710 73	0.710 73
space group	<i>Pna</i> 2 <sub>1</sub>	<i>P4</i> <sub>2</sub> / <i>n</i>
<i>a</i> , Å	20.4302(15)	10.1367(8)
<i>b</i> , Å	8.5552(7)	10.1367(8)
<i>c</i> , Å	9.8549(7)	16.2831(17)
<i>V</i> , Å <sup>3</sup>	1722.5(2)	1673.1(3)
<i>Z</i>	4	4
$\rho_{\text{calcd}}$ , Mg/m <sup>3</sup>	4.958	5.104
$\mu$ (Mo K $\alpha$ ), mm <sup>-1</sup>	25.099	25.839
final <i>R</i> indices	R1 <sup>a</sup> = 0.0295; [ <i>I</i> > 2 $\sigma$ ( <i>I</i> )] wR2 <sup>b</sup> = 0.0489	R1 = 0.0264, wR2 = 0.0568
<i>R</i> indices (all data)	R1 = 0.0432; wR2 = 0.0513	R1 = 0.0358, wR2 = 0.0584

<sup>a</sup> R1 =  $\sum ||F_o| - |F_c|| / \sum |F_o|$ . <sup>b</sup> wR2 =  $[\sum (w(F_o^2 - F_c^2)^2) / \sum (w(F_o^2)^2)]^{1/2}$ .

the structural formula: Cs, 20.7%; U, 37.0%; Mo, 22.4%; O, 19.9% (by difference). During the course of analysis of NDU-1 as well as several other uranyl phases, we found the value of Cs to be ~10% lower than expected, possibly suggesting the standard used was not ideal.

**Crystal Structure Determination.**  $\alpha$ -Cs<sub>2</sub>[(UO<sub>2</sub>)<sub>2</sub>(MoO<sub>4</sub>)<sub>3</sub>]. A single blade-shaped greenish-yellow crystal was mounted on a thin glass fiber for X-ray diffraction analysis. More than a hemisphere of X-ray diffraction data ( $2\theta_{\text{max}} = 56.56^\circ$ ) was collected at room temperature using a Bruker 1K SMART CCD diffractometer with Mo K $\alpha$  radiation. The data were integrated and corrected for absorption using an empirical ellipsoidal model ( $R_{\text{int}} = 0.054$ ) using the Bruker programs SAINT and XPREP.<sup>39,40</sup> The observed systematic absences were consistent with space groups *Pna*2<sub>1</sub> (No. 33) and *Pnam* (No. 62). The structure was solved in both space groups by direct methods and refined on the basis of  $F^2$  for all unique data using the SHELXTL software.<sup>41</sup> Refinement in *Pnam* proved unsatisfactory (no convergence and several nonpositive definite displacement parameters), whereas the *Pna*2<sub>1</sub> model converged to final agreement indices R1 = 0.0295, wR2 = 0.0489, and GOF = 0.919; there were 4015 unique observed reflections ( $I > 2\sigma(I)$ ) and 209 variables. All atoms were refined with anisotropic displacement parameters. As *Pna*2<sub>1</sub> is a noncentrosymmetric space group, care was taken to determine the absolute structure. Details of the data collection and refinement are given in Table 1; atomic coordinates are given in Table 2.

$\beta$ -Cs<sub>2</sub>[(UO<sub>2</sub>)<sub>2</sub>(MoO<sub>4</sub>)<sub>3</sub>]. A yellow plate-shaped crystal was selected and mounted for data collection as above. An empirical absorption correction was applied by modeling the crystal as a (001) plate (resulting  $R_{\text{int}} = 0.067$ ). The structure was solved by direct methods in space group *P4*<sub>2</sub>/*n* (No. 86). An initial refinement of the structure converged to R1 = 0.110, wR2 = 0.295, and GOF = 5.230. The structure model involved disorder of two oxygen atom positions, and the anisotropic displacement parameters for most oxygen atoms were nonpositive definite. Inspection of the calculated and experimental structure factors revealed that many  $F_{\text{exp}}^2$  were

**Table 2.** Atomic Coordinates ( $\times 10^4$ ) and Equivalent Isotropic Displacement Parameters ( $\text{\AA}^2 \times 10^3$ ) for  $\alpha$ -Cs<sub>2</sub>[(UO<sub>2</sub>)<sub>2</sub>(MoO<sub>4</sub>)<sub>3</sub>]<sup>a</sup>

	<i>x</i>	<i>y</i>	<i>z</i>	<i>U</i> (eq)
U(1)	7785(1)	7624(1)	5922(1)	14(1)
U(2)	5264(1)	11664(1)	6791(1)	16(1)
Mo(1)	5341(1)	12448(1)	10591(1)	17(1)
Mo(2)	6346(1)	9802(1)	3787(1)	16(1)
Mo(3)	6927(1)	4094(1)	7365(1)	18(1)
Cs(1)	6441(1)	7844(1)	9377(1)	30(1)
Cs(2)	6064(1)	5056(1)	3902(1)	33(1)
O(1)	6809(3)	8513(10)	4792(8)	27(2)
O(2)	6924(3)	5978(9)	6586(8)	23(2)
O(3)	5313(3)	10385(9)	10720(8)	26(2)
O(4)	5863(4)	11018(11)	4802(8)	34(2)
O(5)	7611(3)	9079(9)	7150(7)	23(2)
O(6)	5664(4)	10158(10)	7694(7)	28(2)
O(7)	5232(3)	13055(9)	8872(7)	24(2)
O(8)	4721(3)	13250(10)	11491(8)	31(2)
O(9)	6913(3)	4325(9)	9158(7)	21(2)
O(10)	6100(3)	13153(10)	11261(7)	22(2)
O(11)	6217(3)	3112(10)	6791(10)	34(2)
O(12)	6863(3)	10968(10)	2781(7)	25(2)
O(13)	7583(4)	3035(9)	6848(10)	34(2)
O(14)	4871(3)	13160(9)	5854(8)	25(2)
O(15)	7979(4)	6150(10)	4735(8)	29(2)
O(16)	5823(4)	8663(10)	2803(8)	32(2)

<sup>a</sup> *U*(eq) is defined as one-third of the trace of the orthogonalized  $U_{ij}$  tensor.

**Table 3.** Selected Bond Lengths (Å) and Angles (deg) for  $\alpha$ -Cs<sub>2</sub>[(UO<sub>2</sub>)<sub>2</sub>(MoO<sub>4</sub>)<sub>3</sub>]

U(1)–O(15)	1.765(8)	U(2)–O(16)	2.451(8)
U(1)–O(5)	1.772(8)	Mo(1)–O(8)	1.691(7)
U(1)–O(2)	2.346(7)	Mo(1)–O(3)	1.770(8)
U(1)–O(10)	2.347(6)	Mo(1)–O(7)	1.786(7)
U(1)–O(9)	2.349(7)	Mo(1)–O(10)	1.790(7)
U(1)–O(1)	2.407(7)	Mo(2)–O(16)	1.740(8)
U(1)–O(12)	2.425(7)	Mo(2)–O(4)	1.748(8)
U(2)–O(6)	1.766(8)	Mo(2)–O(12)	1.758(7)
U(2)–O(14)	1.769(7)	Mo(2)–O(1)	1.759(8)
U(2)–O(11)	2.308(7)	Mo(3)–O(13)	1.697(8)
U(2)–O(3)	2.361(7)	Mo(3)–O(11)	1.768(7)
U(2)–O(7)	2.372(7)	Mo(3)–O(9)	1.778(7)
U(2)–O(4)	2.377(8)	Mo(3)–O(2)	1.785(8)
O(15)–U(1)–O(5)	178.1(4)	Mo(2)–O(12)–U(1)	159.3(4)
O(6)–U(2)–O(14)	178.8(4)	Mo(2)–O(16)–U(2)	147.9(5)
Mo(1)–O(3)–U(2)	142.0(4)	Mo(2)–O(4)–U(2)	154.3(5)
Mo(1)–O(7)–U(2)	132.1(4)	Mo(3)–O(2)–U(1)	131.3(3)
Mo(1)–O(10)–U(1)	136.4(4)	Mo(3)–O(9)–U(1)	131.5(4)
Mo(2)–O(1)–U(1)	154.7(4)	Mo(3)–O(11)–U(2)	161.2(6)

much greater than  $F_{\text{calc}}^2$ , suggesting the crystal studied was twinned. The twin operator [010/100/00 $\bar{1}$ ] was applied, corresponding to merohedral twinning (i.e. when twin operator is a symmetry operator of the crystal system but not of the point group of the crystal).<sup>42</sup> The structure was refined according to the method of Jameson<sup>43</sup> on the basis of  $F^2$  for all unique data, resulting in a substantial improvement of the refinement to R1 = 0.026, wR2 = 0.057, and GOF = 1.024 and a model that did not involve disorder of any atom positions. The refinement indicated two twin components with fractions 58 and 42% of the volume of the crystal. All atoms were refined with anisotropic displacement parameters. Details of the data collection and refinement are given in Table 1; atomic coordinates are in Table 4. Complete listings of bond distances and angles are available for both compounds in CIF format as Supporting Information.

(39) XPREP, V5.1 Data Preparation & Reciprocal Space Exploration; Bruker Analytical X-ray Systems: Madison, WI, 1998.

(40) SAINT, V 5.01 Program for reduction of data collected on Bruker AXS CCD area detector systems; Bruker Analytical X-ray Systems: Madison, WI, 1998.

(41) SHELXTL NT, V5.1 Program suite for solution and refinement of crystal structures; Bruker Analytical X-ray Systems: Madison, WI, 1998.

(42) Herbst-Irmer, R. Twin-Refinement with SHELXL; <http://shelx.uni-ac.gwdg.de/~rherbst/twin.html>.

(43) Jameson, G. B. *Acta Crystallogr.* **1982**, A38, 817–820.

**Table 4.** Atomic Coordinates ( $\times 10^4$ ) and Equivalent Isotropic Displacement Parameters ( $\text{\AA}^2 \times 10^3$ ) for  $\beta$ - $Cs_2[(UO_2)_2(MoO_4)_3]^a$ 

	<i>x</i>	<i>y</i>	<i>z</i>	<i>B</i> (eq)
U(1)	4448(1)	9589(1)	1633(1)	17(1)
Cs(1)	2500	7500	-919(1)	34(1)
Cs(2)	-2500	7500	29(1)	42(1)
Mo(1)	799(1)	9081(1)	1284(1)	19(1)
Mo(2)	2500	2500	2500	19(1)
Mo(3)	7500	7500	2500	17(1)
O(1)	586(6)	9184(6)	2369(4)	25(1)
O(2)	5356(6)	278(7)	814(4)	28(1)
O(3)	3590(6)	8906(6)	2485(5)	28(2)
O(4)	6313(6)	8190(6)	1860(5)	31(2)
O(5)	2313(6)	9881(6)	998(4)	21(2)
O(6)	839(7)	7418(6)	929(4)	23(2)
O(7)	3711(5)	1777(6)	1880(5)	23(2)
O(8)	-515(6)	9860(7)	835(5)	33(2)

<sup>a</sup> *U*(eq) is defined as one-third of the trace of the orthogonalized  $U_{ij}$  tensor.

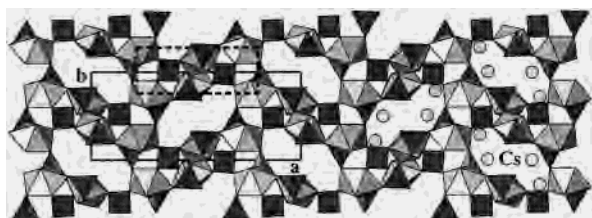


**Figure 1.** Extended framework structure of  $\alpha$ - $Cs_2[(UO_2)_2(MoO_4)_3]$  drawn projected along the *c* axis. Grey pentagonal bipyramids are  $U^{VI}O_7$  polyhedra, whereas dark tetrahedra are  $MoO_4$ . Grey circles are  $Cs^+$  cations. The unit cell is shown (solid line), as is the “chain” of polyhedra (dashed line), for comparison to the  $\beta$  structure in Figure 5.

## Results and Discussion

$\alpha$ - $Cs_2[(UO_2)_2(MoO_4)_3]$ . The structure of  $\alpha$ - $Cs_2[(UO_2)_2(MoO_4)_3]$  (Figure 1) consists of  $U^{VI}O_7$  pentagonal bipyramids that share each of their equatorial anions with  $Mo^{VI}O_4$  tetrahedra, giving rise to a framework of polyhedra. The framework contains two sets of channels: one parallel to [001] with dimensions of approximately  $3.2 \times 10.5 \text{ \AA}$  (as measured from shortest O–O atom center positions) and a

second along [100] with the dimensions  $4.8 \times 4.8 \text{ \AA}$ . The channels contain the Cs(1) and Cs(2) cations that are coordinated by 8 and 10 O atoms, respectively.

The structure contains two symmetrically unique  $U^{6+}$  sites, each of which is bonded to two oxygen atoms (at  $\sim 1.8 \text{ \AA}$ ), giving nearly linear  $(UO_2)^{2+}$  uranyl ions. Each uranyl ion is coordinated by five additional O atoms arranged at the equatorial vertexes of a pentagonal bipyramid. Bond lengths for the  $UO_7$  polyhedra (Table 3) range from 1.76 to 2.45  $\text{\AA}$ , typical values for this polyhedron in many other U–O materials. Each of the equatorial O atoms of the  $UO_7$  polyhedra is further coordinated to one of three unique  $Mo^{6+}$  sites (Figure 2). The  $Mo^{6+}$  cations are tetrahedrally coordinated to four O atoms with bond lengths averaging 1.76  $\text{\AA}$ . The Mo(2) cation is linked to four different  $UO_7$  pentagonal bipyramids, whereas the Mo(1) and Mo(3) sites (Table 2) are linked to only three (Figure 2). The singly coordinated oxygen sites (O(8) and O(3), Table 2) have noticeably shorter than average Mo–O distances of  $\sim 1.70 \text{ \AA}$ . Two unique extraframework Cs atoms are coordinated to 8 and 10 O atoms at distances ranging from 3.07 to 3.67  $\text{\AA}$ . Bond valence sums for the cations calculated on the basis of bond-valence parameters for U(VI)–O,<sup>12</sup> Mo(VI)–O, and Cs(I)–O bonds<sup>14</sup> are 6.06, 6.08, 6.00, 6.10, 6.03, 0.98, and 0.94 vu for U(1), U(2), Mo(1), Mo(2), Mo(3), Cs(1), and Cs(2), respectively. Bond-valence sums at oxygen atoms range from 1.87 to 2.18 vu.

The local structure of  $\alpha$ - $Cs_2[(UO_2)_2(MoO_4)_3]$  may be illustrated using a nodal representation (Figure 2 insets). Each node corresponds to a  $UO_7$  bipyramid (black) or a  $MoO_4$  tetrahedron (white). Nodes are connected if the polyhedra share a common vertex (oxygen atom). The uranyl molybdate structural units can thus be considered as an infinite net where all black vertexes (Figure 2a) are 5-connected and all white vertexes are either 3- or 4-connected (Figure 2b,c respectively) with the ratio of 3-connected vertexes to 4-connected vertexes being 2:1.

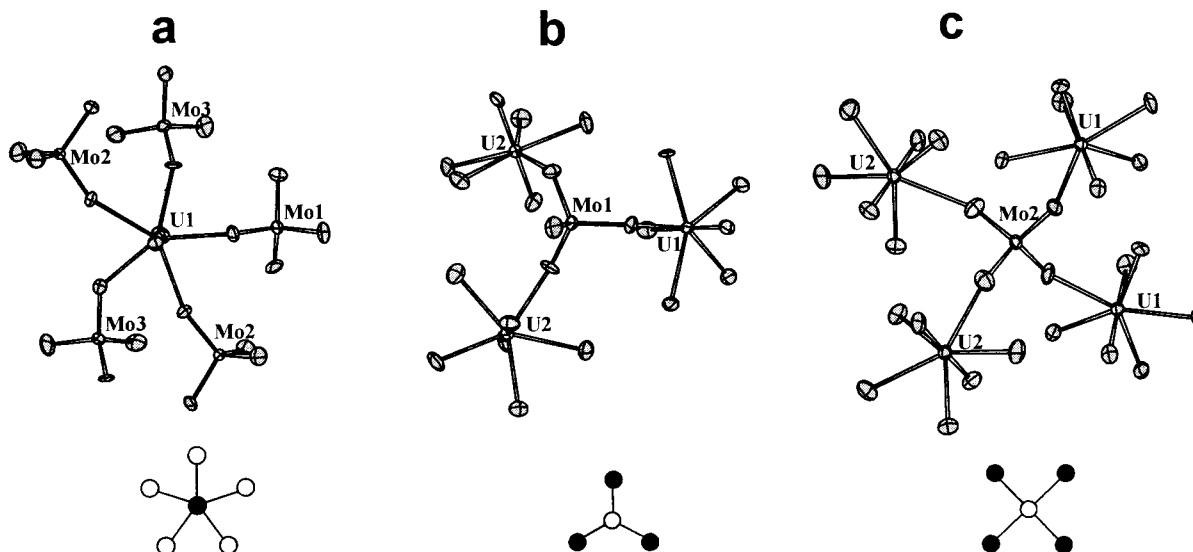


**Figure 2.** Local coordination of U (a), and Mo (b, c) in the structure of  $\alpha$ - $Cs_2[(UO_2)_2(MoO_4)_3]$  shown with atomic displacement ellipsoids (50%) and their nodal representations (insets: white circles = Mo coordination polyhedra; dark circles = U coordination polyhedra).

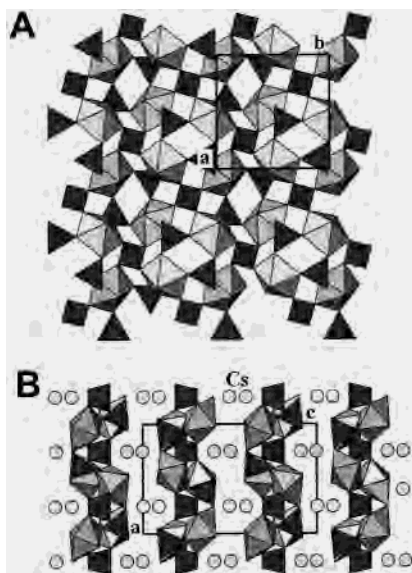


**Figure 3.** Crystal structure of layered  $\beta$ -Cs<sub>2</sub>[(UO<sub>2</sub>)<sub>2</sub>(MoO<sub>4</sub>)<sub>3</sub>] projected along the *c* axis (a) and along the *b* axis (b). The legend is as in Figure 1; the unit cell shown is as a solid line.

**Table 5.** Selected Bond Lengths (Å) and Angles (deg) for  $\beta$ -Cs<sub>2</sub>[(UO<sub>2</sub>)<sub>2</sub>(MoO<sub>4</sub>)<sub>3</sub>]

U(1)–O(2)	1.764(6)	Mo(1)–O(8)	1.713(6)
U(1)–O(3)	1.778(7)	Mo(1)–O(6)	1.783(6)
U(1)–O(6)	2.354(6)	Mo(1)–O(1)	1.783(7)
U(1)–O(1)	2.363(6)	Mo(1)–O(5)	1.797(6)
U(1)–O(7)	2.375(6)	Mo(2)–O(7) × 4	1.750(6)
U(1)–O(4)	2.393(6)	Mo(3)–O(4) × 4	1.738(7)
U(1)–O(5)	2.417(6)		
O(2)–U(1)–O(3)	177.6(3)	Mo(1)–O(6)–U(1)	131.0(4)
Mo(1)–O(1)–U(1)	140.1(3)	Mo(2)–O(7)–U(1)	135.2(3)
Mo(1)–O(5)–U(1)	126.7(3)	Mo(3)–O(4)–U(1)	151.4(5)

**$\beta$ -Cs<sub>2</sub>[(UO<sub>2</sub>)<sub>2</sub>(MoO<sub>4</sub>)<sub>3</sub>].** The synthesis and unit cell parameters of  $\beta$ -Cs<sub>2</sub>[(UO<sub>2</sub>)<sub>2</sub>(MoO<sub>4</sub>)<sub>3</sub>] have been published,<sup>32</sup> but the structure has not been reported. The study by Serezhkin et al. and a later investigation of thermal properties of this phase<sup>33</sup> had inconsistent space group assignments. The structure, reported here for the first time, consists of corrugated sheets of composition [(UO<sub>2</sub>)<sub>2</sub>(MoO<sub>4</sub>)<sub>3</sub>]<sup>2-</sup> shown in Figure 3. The Cs<sup>+</sup> cations are located in the interlayer region and provide charge balance. The shortest O–O distance across the interlayer region is ~3.8 Å (as measured from O(5) to O(2) center position).

Cation coordination polyhedra in the structure of the  $\beta$  phase are similar to those of the  $\alpha$  phase: a single U<sup>6+</sup> cation is in pentagonal bipyramid coordination, and three Mo<sup>6+</sup> cations are tetrahedrally coordinated by O atoms. The UO<sub>7</sub> polyhedron shares each equatorial vertex with MoO<sub>4</sub> tetrahedra. Equatorial U–O bond lengths average 2.38 Å, and Mo–O bond lengths average 1.75 Å (Table 5). Two of the three unique Mo sites are linked to four different U–O polyhedra. The Mo(3) (Table 4) site is linked to only three UO<sub>7</sub> bipyramids. Like the Mo(1) and Mo(3) sites in the  $\alpha$ -phase, the Mo(3) tetrahedron involves a singly coordinated O atom, with a shorter than average Mo(3)–O distance of ~1.71 Å. Bond valence sums at the cations calculated on the basis of bond-valence parameters for U(VI)–O,<sup>12</sup> Mo(VI)–O, and Cs–O bonds<sup>14</sup> are 6.02, 5.83, 6.12, 6.32, 0.84,

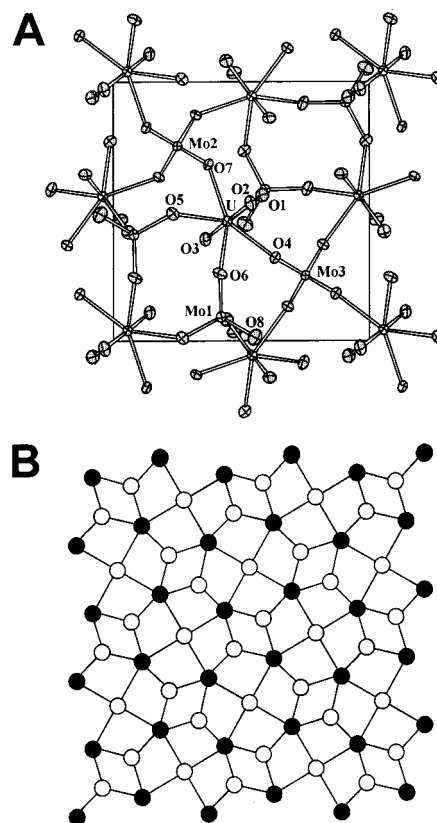


**Figure 4.** ORTEP (50% ellipsoids) view of the sheet of U, Mo, and O atoms in the structure of  $\beta$ -Cs<sub>2</sub>[(UO<sub>2</sub>)<sub>2</sub>(MoO<sub>4</sub>)<sub>3</sub>] (a) and nodal representations. The scheme for nodal representation is as in Figure 2.

and 0.75 vu for U, Mo(1), Mo(2), Mo(3), Cs(1), and Cs(2), respectively. Bond-valence sums at oxygen atoms range from 1.81 to 2.19 vu.

As in the  $\alpha$  phase, the topology of the  $\beta$  phase can be described in terms of a nodal representation (Figure 4b). In the nodal representation, each U site is connected to five Mo sites, whereas two of the Mo sites are 4-connected and one is only 3-connected.

The topology of the [(UO<sub>2</sub>)<sub>2</sub>(MoO<sub>4</sub>)<sub>3</sub>]<sup>2-</sup> sheet in the  $\beta$ -phase is identical to that of the [(UO<sub>2</sub>)<sub>2</sub>(SO<sub>4</sub>)<sub>3</sub>]<sup>2-</sup> sheet found in Cs<sub>2</sub>[(UO<sub>2</sub>)<sub>2</sub>(SO<sub>4</sub>)<sub>3</sub>]<sup>44</sup> if one substitutes the SO<sub>4</sub> for MoO<sub>4</sub> tetrahedra. The space group reported for Cs<sub>2</sub>[(UO<sub>2</sub>)<sub>2</sub>(SO<sub>4</sub>)<sub>3</sub>] is *P*4<sub>2</sub>*m* (No. 113) suggests that it is not isostructural with  $\beta$ -Cs<sub>2</sub>[(UO<sub>2</sub>)<sub>2</sub>(MoO<sub>4</sub>)<sub>3</sub>]. It should be noted, however, that at least for the U–Mo phase, the correct space group determination was complicated by twinning of the crystals. Twinning of the crystal examined by Ross and Evans could explain the relatively high agreement index (*R* = 0.11) and perhaps the different space group assigned for Cs<sub>2</sub>[(UO<sub>2</sub>)<sub>2</sub>(SO<sub>4</sub>)<sub>3</sub>].

**Relationships between  $\alpha$  and  $\beta$  Polymorphs.** The structures of both the  $\alpha$  and  $\beta$  phases can be described in terms of cross-linked chains of UO<sub>7</sub> pentagonal bipyramids and MoO<sub>4</sub> tetrahedra (Figure 5). The chains are linked in two dimensions in the  $\beta$  phase to form infinite sheets. The same chain topology in the  $\alpha$  phase is linked to form a three-dimensional framework. In this case the chains extend

(44) Ross, M.; Evans, H. T. *J. Inorg. Nucl. Chem* **1960**, *15*, 338–351.

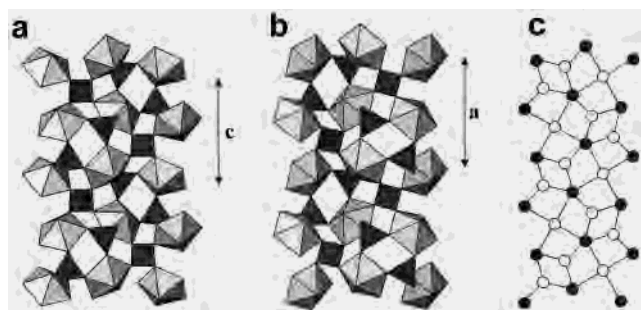


**Figure 5.** Topologically related chains of  $\text{UO}_7$  pentagonal bipyramids and  $\text{MoO}_4$  tetrahedra in the crystal structures of  $\alpha\text{-Cs}_2[(\text{UO}_2)_2(\text{MoO}_4)_3]$  (a),  $\beta\text{-Cs}_2[(\text{UO}_2)_2(\text{MoO}_4)_3]$  (b), and their nodal representation (c).

parallel to the  $c$  axis and are cross-linked along approximately  $[\bar{1}10]$  to produce a framework (Figure 1). The chain in the structure of the  $\alpha$  phase has a translation period of 9.85 Å, which is shorter than the analogous chains in the  $\beta$  phase, which have a translation period of 10.14 Å (Figure 5).

### Discussion

The structures of the two polymorphs of  $\text{Cs}_2[(\text{UO}_2)_2(\text{MoO}_4)_3]$  further demonstrate the structural complexity and variability of uranyl compounds. Unlike most uranyl phases,<sup>12</sup> these compounds do not involve polymerization of uranyl polyhedra with other uranyl polyhedra, nor do they involve the sharing of polyhedral edges between polyhedra of higher bond valence. The lack of polymerization of uranyl polyhedra with other uranyl polyhedra in general enhances the likelihood of connectivities involving themes other than sheets. The sharing of vertexes only between uranyl polyhedra and tetrahedra results in more structural flexibility than where the sharing of edges is involved, which increases the likelihood of a given composition adopting a structural

connectivity involving a framework of polyhedra. As a result of these factors, the structures of uranyl compounds containing tetrahedrally coordinated hexavalent cations (Mo, S, Cr) show more structural diversity than uranyl compounds in general; such compounds are more likely to adopt structures based upon finite clusters, chains, or frameworks of polyhedra.<sup>45</sup> This observation is significant to our goals of producing microporous uranyl molybdate structures.

Experiments are in progress to determine any ion-exchange capabilities of these materials. Syntheses using different cations in the reaction mixture (e.g.  $\text{K}^+$  and  $\text{NH}_4^+$ ), however, result in a markedly different 3-dimensional framework structure. This material will be the subject of a forthcoming paper.

**Acknowledgment.** This research was supported by the Environmental Management Sciences Program of the United States Department of Energy (Grant DE-FG07-97ER14820) and by an NSF-NATO Fellowship in Science and Engineering that supports S.V.K. (Grant DGE99-03354). S.V.K. thanks the Russian Foundation for Basic Research (RFBR) for additional financial support (Grant 01-05-64883). C.L.C. is grateful to the George Washington University for start-up funding. We are grateful to Dr. Ian Steele of the University of Chicago for the electron microprobe analysis.

**Supporting Information Available:** A file of X-ray crystallographic data for  $\alpha$ - and  $\beta$ - $\text{Cs}_2[(\text{UO}_2)_2(\text{MoO}_4)_3]$  in CIF format. This material is available free of charge via the Internet at <http://pubs.acs.org>.

IC010345Y

(45) Burns, P. C. Structures of uranyl minerals and compounds containing tetrahedrally coordinated hexavalent cations. In *Eleventh Annual V. M. Goldschmidt Conference*; Lunar and Planetary Institute: Houston, TX, 2001; Abstract No. 3263, LPI Contribution No. 1088 (CD-ROM).